EXPERIMENTAL AND NUMERICAL EVALUATION OF FATIGUE CRACK INITIATION AND PROPAGATION FOR IN738LC AT 850°C

B. Fedelich*, H. Frenz*, W. Österle* and K. Stark*

Interrupted LCF-tests at 850°C for Inconel 738LC have been carried out and the specimens have been intensively examined by REM to quantify the evolution of fatigue damage. Surface crack nucleation at oxidized grain boundaries and coalescence of neighbouring flaws occured during the whole experiment. An anomalous fast single crack growth is observed just after nucleation, followed by a relative stagnation of the propagation in absence of coalescence. A statistical model is proposed that describes these phenomena. It leads to an integro-differential equation for the crack density $f(c,n)$ after n cycles, similar to the Bolzmann equation which describes the collision of molecules in a dilute gas.

EXPERIMENTAL PROCEDURE

After the standard heat treatment, (2 hours at 1120 °C/ air cooling; 24 hours at 845°C in argon or vacuum/cooling to room temperature) the alloy IN 738LC has a dendritic structure with large carbides, undissolved primary γ/γ'-nodules and casting pores along the grain and the dentrite boundaries. The volume fraction of the γ'-phase in the alloy is about 45 %. Cylindrical smooth specimens with 9 mm diameter and 35 mm gauge length were used. Interrupted LCF-tests (ε = +/- 0,6 %, $\dot{\varepsilon} = 10^{-3} s^{-1}$, sinusoidal waveform) were carried out with a closed-loop INSTRON system under strain control at 850 °C in air. After interruptions, the specimens were extensively examined by REM and by replica-technique in order to quantify the evolution of fatigue damage (Stark, (1)). The crack length was defined as the length perpendicular to the load axis.

* Bundesanstalt für Materialforschung und -prüfung (BAM)
Unter den Eichen 87, 12205 Berlin, Germany.

EXPERIMENTAL RESULTS

Crack nucleation

The first small cracks were found after less than 5% of the total life. Surface cracks nucleation occured essentially along oxidized grain boundaries, at primary eutectic γ/γ'-nodules and by cracking of brittle MC-carbides (Fedelich et al., (2)). The oxidation mechanism of MC-carbides is quite different from that of the metal matrix, as reported by Litz et al. (3). The metal matrix forms a protective layer rich in Cr_2O_3 and the carbides a non protective scale growing at the oxide-carbide interface. The oxidation causes a large volume increase. The different oxidation rates of matrix and carbides, the large volume increase during the oxidation of the carbides and the scale growth at the oxide/carbide interface lead to an outward movement of the carbide oxidation products. This mechanism causes high shear strains at the interface Cr_2O_3/oxidized carbid. The consequence is repeated cracking in these regions, giving aggressiv components a chance to penetrate the metal matrix, thereby causing internal corrosion processes. Cracks at the oxidized carbides lead to preferential internal corrosion around oxidized carbide particles (3). The investigation revealed no signs of grain boundary cavitation.

Crack growth and coalescence

On the specimen surface, the crack propagation occured mainly along the grain boundaries (2). Immediately after nucleation, cracks grow perpendicular to the load axis. After a relatively short period of intergranular deep crack growth, the propagation becomes transgranular, as also found at 900°C by Jianting et al. (4). On the oxidized fracture surfaces, striations were found, which indicate that crack growth occurs according to the crack-tip blunting mechanism. The ratio of surface crack length $2a$ and crack depth c was between 2 and 2.5. On the specimen surface, networks of slip planes were observed ahead of the tip of some larger cracks (Fig. 1) that reflect the high plastic deformations in these zones. Fig. 2 shows the evolution of the surface lengths of some representative cracks. It demonstrates the very pronounced effect of coalescence. Mostly, as also observed by Forsyth (5), linking occurs between two cracks with a small offset which grow with their closest tips passing one another before deviating and growing towards each other (Fig. 3-4). Cracks coalescence becomes more and more important as the number of cycles increases. It was observed with cracks of all sizes and at all stages of growth, but the probability of two cracks being close enough to link up increases with cracks density and size. On the other hand, cracks that didn't undergo coalescence were often found to stagnate after a short period of fast propagation.

Figure 1. Plastic deformations at a crack tip.

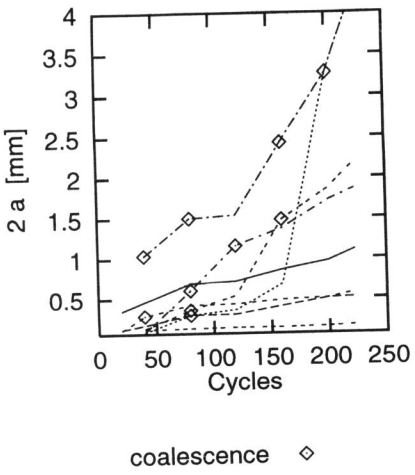

Figure 2. Crack growth with and without coalescence.

Figure 3. Two cracks before ...

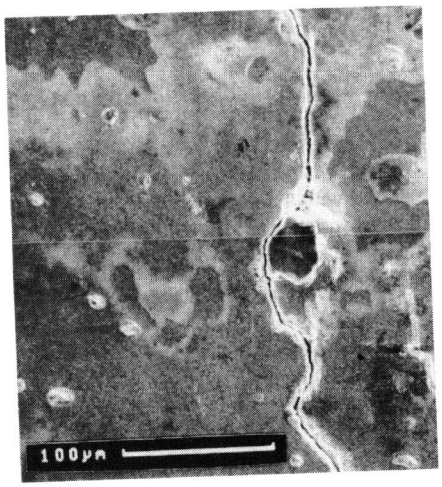

Figure 4. ...and after coalescence.

MODELLING OF CRACK GROWTH UNDER LCF LOADING

A simplified model of crack tip plasticity for small cracks

An extension of the Dugdale/Barenblatt model (6) by Navarro and de Los Rios (7) has been used to account for local heterogeneities at the crack tip. We denote σ the tension at infinity and $2c$ the crack length (Fig. 5). The behaviour of the grains ahead of the crack tip is represented by piece-wise constant cohesion stresses $S(x) = S_i$ acting on limited ranges L_i of the x-axis. In the symmetrical case, and if $c \le L_1$, the length of the plastic zone D is given by:

$$\sigma - \frac{2}{\pi} \sum_{i=1}^{k} S_i \left(\arcsin\left(\frac{a_i}{c+D} \right) - \arcsin\left(\frac{a_{i-1}}{c+D} \right) \right) = 0 \qquad (1)$$

where: $a_0 = c$, $a_1 = L_1$, $a_i = a_{i-1} + L_i$ *for* $i = 2 \ldots k-1$, $a_k = c + D$. This model may be adapted to LCF loading as proposed by Tomkins (8): there is a zone at the crack tip that is highly plastically strained, whereas in the bulk-material plastic strains are of several order of magnitude lower and may be neglected. The amount of crack growth in one cycle is assumed to be:

$$v(c) = \frac{dc}{dn} = \alpha \, \Delta\varepsilon_p \, D(c, \sigma, S_i, L_i) \qquad (2)$$

where D is given by equation (1), $\Delta\varepsilon_p$ is the plastic strain amplitude and σ the maximum tensile stress during a cycle. A correction factor $\alpha = 0.51$ has been used, following Dowling (9), to account for half-circular surface cracks of radius c.

A statistical model for collective crack growth

We assume that linking of two cracks occurs if the highly strained plastic zones overlap, when the crack tips are in opposition (Fig. 6) and that the new crack is half-circular with a radius: $c = c' + c''$. We suppose now that crack nucleation is continuous with a constant intensity $H \; p^0(c_0)$: H is the density of flaws created per cycle and $p^0(c_0)$ the probability density function for the initial size. The distribution function $f(c,n)$ that gives the surface density of cracks of length c after n cycles obeys the following balance law:

$$\frac{\partial f}{\partial n} + \frac{\partial f v}{\partial c} = H p^0(c) + \frac{1}{2} \int_0^c f(c') \, f(c-c') \, \Omega(c', c-c') \, dc' - \int_0^{+\infty} f(c) \, f(c') \, \Omega(c, c') \, dc' \qquad (3)$$

with: $\Omega(c', c'') = 4/\sqrt{2} \; \alpha \; \Delta\varepsilon_p \; (D' + D'')^2$ and the initial condition: $f(c;0) = 0$.

The crack growth rate v is given by equation (2).

Results

Assuming a grain size $L_i = 0.8mm$, $\sigma = 600\,MPa$, and $\Delta\varepsilon_p/2 = 0.0023$, the cohesion stresses S_i were fitted separately for 14 cracks that didn't coalesce. Then, the parameters in (2) were set to the mean values $<S_1> = 745\,MPa$, $<S_2> = 789\,MPa$, $<S_3> = 956\,MPa$ respectively. The initial crack lengths were supposed to be distributed according to a Weibull law. With a constant crack nucleation rate $H = 0.03\,/mm^2/cycle$, the crack density $f(c,n)$ has been calculated after 200 cycles (Fig. 7) which is roughly the fatigue life under these loading conditions. Note that the experimental data concerns all flaws found in the examined area (over 200 cracks) and not only those that were used for the model calibration. The total crack density $F(n) = \int_0^\infty f(c,n)\,dc$ vs. the number of cycles is plotted in Fig. 8. A saturation is observed that is also correctly predicted by the model and corresponds approximatively to the end of life of the specimen.

Acknowledgement- This research work is part of the project Sfb339 "Turbine blades and disks" and the financial support of the Deutsche Forschungsgemeinschaft DFG is gratefully acknowledged.

REFERENCES

(1) Stark, K., "Experimentelle Quantifizierung der Schädigungsentwicklung an der Nickelbasis-Superlegierung IN738LC", Diplomarbeit, Technical University Berlin, 1995.
(2) Fedelich, B., Frenz, H., Österle, W. and Stark, K., "A stochastic model for LCF small cracks growth in a Nickel-base Superalloy", Proceedings of Fatigue `96, Berlin, 1996.
(3) Litz, J., Rahmel, A., and Schorr, M., Oxidation of Metals, Vol. 30, No. 1/2, 1988, pp. 95-105.
(4) Jianting, G., Ranucci, D. and Strocchi, P.M., Int. J. Fatigue, Vol. 6, No. 2, 1984, pp. 95-99.
(5) Forsyth, P.J.E., Int. J. Fatigue, Vol. 5, 1983, pp. 3-14.
(6) Dugdale, D.S., J. Mech. Phys. Solids, Vol. 8, 1960, pp. 100-104.
(7) Navarro, A. and De Los Rios E. R., Phil. Magazine, Vol. 57, No. 1, 1988, pp. 43-50.
(8) Tomkins, B., Phil. Magazine, Vol. 18, 1968, pp. 1041-1066.
(9) Dowling, N. E., ASTM STP 637, 1977, pp. 97-121.

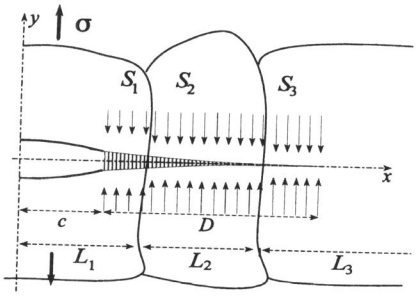

Figure 5. Multizone Dugdale/ Barenblatt crack model.

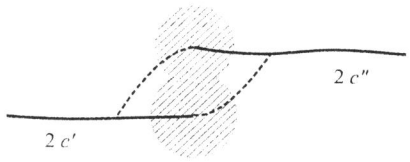

Figure 6. Coalescence of two micro-cracks.

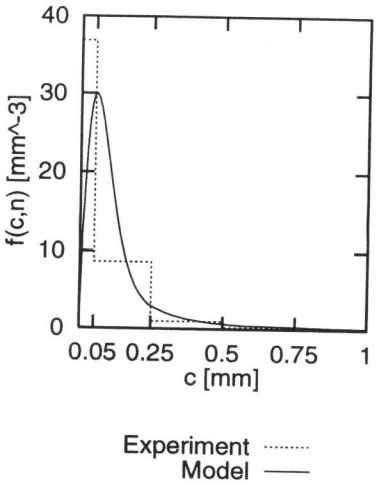

Figure 7. Crack length distribution after 200 cycles.

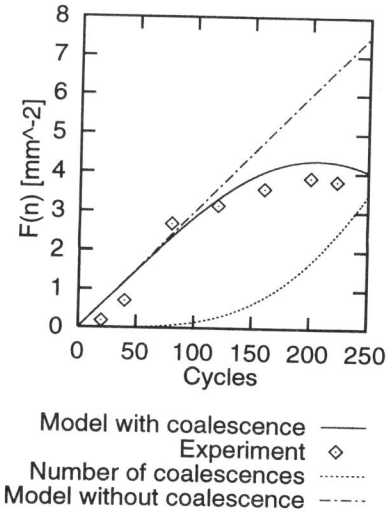

Figure 8. Evolution of the total crack density.